

Nonrelativistic Effective Field Theory with a Resonance Field

J. B. Habashi,¹ S. Fleming,¹ and U. van Kolck^{2,1}

¹*Department of Physics, University of Arizona, Tucson, AZ 85721, USA*

²*Université Paris-Saclay, CNRS/IN2P3, IJCLab, 91405 Orsay, France*

(Dated: March 1, 2022)

We discuss shallow resonances in the nonrelativistic scattering of two particles using an effective field theory (EFT) that includes an auxiliary field with the quantum numbers of the resonance. We construct the manifestly renormalized scattering amplitude up to next-to-leading order in a systematic expansion. For a narrow resonance, the amplitude is perturbative except in the immediate vicinity of the resonance poles. It naturally has a zero in the low-energy region, analogous to the Ramsauer-Townsend effect. For a broad resonance, the leading-order amplitude is nonperturbative almost everywhere in the regime of validity of the EFT. We regain the results of an EFT without the auxiliary field, which is equivalent to the effective-range expansion with large scattering length and effective range. We also consider an additional fine tuning leading to a low-energy amplitude zero even for a broad resonance. We show that in all cases the requirement of renormalizability when the auxiliary field is not a ghost ensures the resonance poles are in the lower half of the complex momentum plane, as expected by other arguments. The systematic character of the EFT expansion is exemplified with a toy model serving as underlying theory.

I. INTRODUCTION

Information about quantum mechanical systems comes from two-body scattering experiments, a prominent feature of which are resonance peaks. Resonances typically reflect interactions that are not strong enough to produce a bound or virtual state, as for nucleon-alpha particle and alpha-alpha scattering. When the resonance is visible at energies that are small compared to those of the break-up of the scattering particles, we can describe the reaction through an effective field theory (EFT) with those particles as degrees of freedom — for a recent, comprehensive review, see Ref. [1].

A resonance peak can be associated with a pole in the S matrix near the positive energy axis of the complex energy plane. An EFT aims for a model-independent description of the S matrix at low energies, which is constrained only by symmetries. A shallow state is associated with a momentum much smaller than the inverse of the range of the interaction and requires only contact interactions. Including all possible contact interactions with an arbitrary number of derivatives ensures that the EFT can describe the low-energy S matrix of a finite-range interaction without the need to know the exact form of the interaction at short distances. Maintaining model independence at the quantum-mechanical level demands renormalization, that is, insensitivity to the regularization needed to yield finite observables. By their very nature, S -matrix poles are non-perturbative and require a summation of Feynman diagrams to all loop orders for a subset of interactions. The challenge for EFTs that include shallow poles is to produce a renormalized and realistic leading-order amplitude while treating subleading interactions in a systematic, perturbative expansion.

The EFT for a single shallow pole on the positive or negative imaginary axis in the complex momentum plane — representing, respectively, a bound or virtual state — is well understood [2–5]. This EFT applies when the two-body scattering length is much larger than the effective range, such as for nucleons or ${}^4\text{He}$ atoms — for an introduction, see Ref. [6]. These are the simplest “halo” states — intrinsically quantum-mechanical states with size larger than the range of the underlying interaction. The EFT for shallow resonances, which can be thought of as unbound halo states, has not been as fully developed.

The first formulation of an EFT for nonrelativistic resonances was proposed [7, 8] for neutron-alpha p -wave scattering. It was argued that at least two parameters are needed for renormalization, which was carried out with an auxiliary “dimer” field [9] having the quantum numbers of the resonance, the ground state of the ${}^5\text{He}$ nucleus. The theory was generalized to narrow resonances — those very close to real energies — in any partial wave in Ref. [8] and applied, in the presence of the Coulomb interaction, to the s -wave resonance (the ground state of the ${}^8\text{Be}$ nucleus) in alpha-alpha scattering in Ref. [10]. For the case of the Delta resonance in Compton scattering on the nucleon, a similar idea was implemented independently in Ref. [11] and reformulated along the lines of Ref. [8] for p -wave pion-nucleon scattering in Ref. [12]. The importance of the non-resonant background in the description of narrow s -wave resonances was emphasized in Ref. [13], with subleading corrections further investigated in Ref. [14].

The dimer field is quite useful as the energy-dependent interaction it produces is equivalent to the resummation of a subset of contact interactions. Recently we presented an equivalent momentum-dependent description of an s -wave resonance without the dimer field [15]. It accounts well for two low-energy poles produced by a generic short-range potential, reproducing the first two terms in the effective-range expansion with scattering length and effective range of

comparable size. This includes a broad resonance represented by a pair of poles of the S matrix that do not lie close to the real axis and are sometimes not considered “true” resonances. It does not naturally accommodate a narrow resonance and its background.

Here we extend the EFT for s -wave resonances to cover both broad and narrow resonances with a dimer field. After a brief description of the EFT with a dimer field in Sec. II, we show in Sec. III that the dimer formulation of broad s -wave resonances gives indeed the same on-shell results as momentum-dependent interactions [15]. In Sec. IV we revisit the case of narrow resonances and point out that the background introduced in Ref. [13] leads to sufficiently strong energy dependence for the scattering amplitude to admit a zero in the low-energy region. We also correct the renormalization procedure of a calculation found in the literature [14]. Section V is dedicated to a toy model that illustrates some of the aspects of the EFT for narrow resonances. In Sec. VI the case is considered of an additional fine tuning leading to an amplitude zero in presence of a broad resonance. We conclude in Sec. VII.

II. EFT WITH A RESONANCE FIELD

The central paradigm of EFT is separation of scales: low-energy degrees of freedom (at a scale M_{lo}) cannot resolve high-energy physics (at a scale M_{hi}). The latter is encoded in the parameters — “low-energy constants” (LECs) — of all the interactions among the low-energy degrees of freedom which are allowed by symmetries. The degrees of freedom in EFT are fields that incorporate the creation and annihilation of particles. The simplest way to account for symmetries is through a Lagrangian, whose infinite number of terms are organized according to the magnitude of their effects on observables. This “power counting” (PC) underlines the expansion of observables in powers of the ratio Q/M_{hi} , where $Q \sim M_{lo} \ll M_{hi}$ is the characteristic external momentum of a process. We refer to successive terms in the expansion in Q/M_{hi} as leading order (LO), next-to-leading order (NLO), *etc.* The EFT breaks down at M_{hi} .

We construct the most general two-body Lagrangian which for simplicity we assume to be invariant under time reversal, parity, and Lorentz transformations, limiting ourselves to a single stable particle species. At energies below the particle mass m , Lorentz invariance is most easily implemented in a Q/m expansion, which gives rise to a nonrelativistic expansion. Pair production cannot occur and particle number is conserved. One can use a field ψ that involves only the annihilation of particles. The Lagrangian is Hermitian and all LECs are real. At very low energies the dominant partial wave is s , and we restrict ourselves to this wave here. Generalization to other waves is straightforward but tedious. We are interested in the case where there is a shallow resonance and introduce a dimer auxiliary field d [9, 16] with its quantum numbers and a residual mass Δ . The most general Lagrangian is then

$$\begin{aligned} \mathcal{L} = & \psi^\dagger \left(i \frac{\partial}{\partial t} + \frac{\vec{\nabla}^2}{2m} \right) \psi + d^\dagger \left(i \frac{\partial}{\partial t} + \frac{\vec{\nabla}^2}{4m} - \Delta \right) d \\ & + \sqrt{\frac{4\pi}{m}} \frac{g_0}{4} (d^\dagger \psi \psi + \psi^\dagger \psi^\dagger d) - \frac{4\pi}{m} C_0 (\psi^\dagger \psi) (\psi^\dagger \psi) \\ & + \sqrt{\frac{4\pi}{m}} \frac{g_2}{4} \left[d^\dagger \left(\psi \overleftrightarrow{\nabla}^2 \psi \right) + \left(\psi \overleftrightarrow{\nabla}^2 \psi \right)^\dagger d \right] + \frac{4\pi}{m} \frac{C_2}{8} \left[(\psi \psi)^\dagger \left(\psi \overleftrightarrow{\nabla}^2 \psi \right) + \left(\psi \overleftrightarrow{\nabla}^2 \psi \right)^\dagger (\psi \psi) \right] \\ & + \dots, \end{aligned} \quad (1)$$

where C_{2n} and g_{2n} are real LECs and “ \dots ” indicates terms with additional fields or derivatives. There is a certain redundancy in the Lagrangian (1), since when one integrates out d one obtains a string of four- ψ interactions of the form already present in \mathcal{L} [17]. However, these terms are all correlated in a way that is explicit only once the dimer field is kept. The four-field interactions retained in Eq. (1) can be thought of as the uncorrelated part of these interactions. In other situations one might need to capture a different correlation by making the dimer a ghost field with a negative kinetic term [9].

With the standard rules of quantum field theory the Lagrangian (1) leads to an infinite number of contributions to the T matrix. We want to organize these contributions at energy $E \equiv k^2/m$ in an expansion

$$T(k) = T^{(0)}(k) + T^{(1)}(k) + \dots \quad (2)$$

or, alternatively,

$$\frac{1}{T(k)} = \frac{1}{T^{(0)}(k)} \left(1 - \frac{T^{(1)}(k)}{T^{(0)}(k)} + \dots \right), \quad (3)$$

where $T^{(n)}$ represents a term of relative $\mathcal{O}(Q^n/M_{hi}^n)$. The S matrix is then obtained from

$$S(k) = 1 - \frac{imk}{2\pi} T(k). \quad (4)$$

Note that, except at $k = 0$, the poles of S and T are the same. In the cases of interest here, $S(k)$ has $N = 2, 3$ (complex) poles denoted by k_n , and it can be written as (*cf.* Refs. [18–20])

$$S(k) = (-1)^N \exp(2i\phi(k)) \prod_{n=1}^N \frac{k - k_n^*}{k - k_n}, \quad (5)$$

where $\phi(k)$ is a smooth background phase. We are particularly concerned with shallow resonances, which consist of a pair of poles in the complex momentum plane,

$$k_{\pm} = \pm k_R - ik_I, \quad (6)$$

with real $k_{R,I} > 0$. In the absence of other shallow poles, the S matrix can be expressed in terms of the resonance energy and (energy-dependent) width, respectively

$$E_R = \frac{1}{m} (k_R^2 + k_I^2), \quad \Gamma(E) = 4k_I \sqrt{\frac{E}{m}}, \quad (7)$$

as

$$S(E) = \exp(2i\phi(E)) \frac{E - E_R - i\Gamma(E)/2}{E - E_R + i\Gamma(E)/2}. \quad (8)$$

To obtain T , one first needs to regulate the theory. We choose the conceptually simplest regulator, a cutoff Λ in momentum space. Results should be independent of regulator choice, which is achieved by the process of renormalization. At each order in the expansion, positive powers of Λ arising from the loops should be removed from observables by the cutoff dependence of a finite number of bare LECs in \mathcal{L} . This fixes the cutoff dependence of the LEC at that order. The finite combinations of bare LECs and loops that remain is then fitted to an equal number of inputs. When the underlying theory is known, one can match its results for a certain number of observables. When the underlying theory is not known or cannot be calculated, one can use experimental data instead. In either case, since at each order only a finite number of LECs is present, observables not used in the fit can be predicted. Higher-order contributions will eventually affect not only these observables but also observables that were already used as input at lower orders. When that happens a LEC that was fixed needs to be changed. It is therefore convenient to split a LEC as

$$\alpha(\Lambda) = \alpha^{(0)}(\Lambda) + \alpha^{(1)}(\Lambda) + \dots, \quad (9)$$

where $\alpha^{(n)}(\Lambda)$ is fixed at order n in the expansion.

This procedure is standard and applied to any EFT — for example, applications to nuclear physics can be found in Ref. [1]. What depends on the physical situation is the PC that determines which interactions appear at each order. From naive dimensional analysis (NDA) — for a review see Ref. [21] — we expect that $\Delta = \mathcal{O}(M_{hi}^2/m)$, $g_{2n} = \mathcal{O}(m^{-1/2} M_{hi}^{1/2-n})$, and $C_{2n} = \mathcal{O}(M_{hi}^{-2n-1})$. In this case the expansion (2) is obtained from strict perturbation theory and there are no poles within the regime of applicability of the EFT.

Below we consider the various deviations from NDA that can give rise to a low-energy resonance, $E_R \ll \mathcal{O}(M_{hi}^2/m)$. This can be achieved with

$$\Delta^{(0)} = \mathcal{O}\left(\frac{M_{lo}^2}{m}\right) \quad (10)$$

because then both kinetic and residual mass terms of the dimer are expected to have similar sizes for momenta $Q = \mathcal{O}(M_{lo})$. Already the bare dimer propagator,

$$D_0^{(0)}(k) = \frac{1}{k^2/m - \Delta^{(0)} + i\epsilon}, \quad (11)$$

displays two poles. With two particle legs attached at each end, $4\pi g_0^{(0)2} D_0^{(0)}(k)/m$ is an energy-dependent potential. Whether this potential can be treated in perturbation theory or instead quantum corrections are important and move

the poles significantly will depend on the scaling of g_0 . The two parameters $\Delta^{(0)}$ and $g_0^{(0)}$ will determine the energy E_R and decay width Γ of the resonance.

The first quantum correction $D_1(k)$ to the bare dimer propagator (11) consists of the one-loop dimer self-energy, that is, an insertion of a particle bubble,

$$\frac{D_1(k)}{D_0^{(0)}(k)} = -g_0^{(0)2} D_0^{(0)}(k) I_0(k), \quad (12)$$

where the loop gives rise to

$$I_0 = L_1 + ik + L_{-1}k^2 + L_{-3}k^4 + \dots, \quad (13)$$

$$L_n \equiv \theta_n \Lambda^n. \quad (14)$$

Here θ_n are pure numbers whose values depend on the regularization scheme. For a sharp momentum cutoff, for example, $\theta_n = 2/n\pi$.

The cutoff-dependent terms are eventually removed by renormalization. As in any EFT, the loop contribution that is not affected by a LEC is the non-analytic term, here the ik in Eq. (13). Thus it gives an estimate of the relative importance of $D_1(k)$,

$$\frac{D_1(k)}{D_0^{(0)}(k)} = \mathcal{O}\left(\frac{mg_0^{(0)2}}{M_{lo}}\right), \quad (15)$$

for momenta $Q \sim M_{lo}$. Additional loop insertions in between bare dimer propagators bring in additional powers of this factor. The size of $g_0^{(0)}$ determines whether the series of loops in the dimer propagator needs to be resummed or not, leading to a broad or narrow resonance, respectively. In all of the PCs we consider, we assume an additional suppression in interactions with LECs $g_{2n>0}$ relative to g_0 , which is given by NDA,

$$g_{2n>0} = \mathcal{O}\left(\frac{g_0}{M_{hi}^{2n}}\right), \quad (16)$$

so they enter at $N^2\text{LO}$ or higher. In calculations up to NLO, we see no renormalization enhancement over this estimate. If such an enhancement is found at higher orders, it can easily be accounted for.

As we will see, another interesting feature of the T matrix can appear depending on the scaling of C_0 : a point on the real momentum axis where the amplitude vanishes, which is analogous to the Ramsauer-Townsend effect [22, 23]. The scaling of the LECs $C_{2n>0}$ will depart from NDA if the scaling of C_0 does. When C_0 satisfies NDA, we assume $C_{2n>0}$ does as well.

III. BROAD RESONANCE

In certain regions of parameter space, a potential consisting of an attractive well surrounded by a repulsive barrier of range R displays a pair of low-energy poles with complex momenta of magnitude $|k| \ll R^{-1}$. If the attraction is not too strong, the two poles are at momenta (6) with $k_I \sim k_R = \mathcal{O}(M_{lo}) > 0$. In this case the resonance width and energy are comparable $\Gamma \sim E_R = \mathcal{O}(M_{lo}^2/m)$.

Since the imaginary part of the complex pole momentum comes from loop integration, regardless of the detailed form of the underlying interactions we must have

$$g_0^{(0)} = \mathcal{O}\left(\sqrt{\frac{M_{lo}}{m}}\right). \quad (17)$$

At LO we then need to resum the one-loop dimer self-energy as in Fig. 1, resulting in the dressed dimer propagator

$$D^{(0)}(k) = \frac{D_0^{(0)}(k)}{1 + g_0^{(0)2} D_0^{(0)}(k) I_0(k)}. \quad (18)$$

This propagator contains the small scale M_{lo} associated with a low-energy resonance.

Here we assume that C_0 is not enhanced with respect to NDA,

$$C_0^{(0)} = 0, \quad C_0^{(1)} = \mathcal{O}\left(\frac{1}{M_{hi}}\right). \quad (19)$$

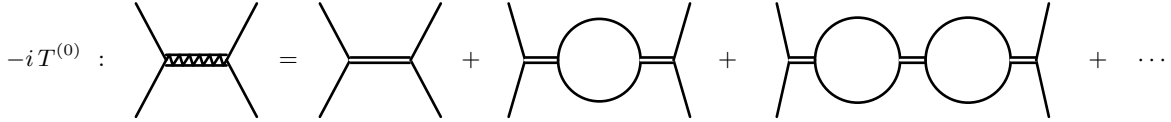


FIG. 1: Leading-order T matrix for a broad resonance in terms of the dressed dimer propagator (shaded double line) arising from the resummation of diagrams with successive particle (solid line) bubble insertions in a bare dimer propagator (double line).

This scaling arises naturally in a simple model [15]. With this assumption the LO T matrix is simply

$$T^{(0)}(k) = \frac{4\pi}{m} g_0^{(0)2} D^{(0)}(k) = -\frac{4\pi}{m} \left(-\frac{1}{a_0} + \frac{r_0}{2} k^2 - ik - L_{-1} k^2 + \dots \right)^{-1}. \quad (20)$$

In Eq. (20) we have absorbed the cutoff dependence from L_1 (which diverges if $\Lambda \rightarrow \infty$) in the bare LEC $\Delta^{(0)}(\Lambda)$, while $g_0^{(0)}$ does not run with the cutoff. We have defined the renormalized parameters a_0^{-1} and r_0 through

$$\Delta^{(0)}(\Lambda) = -\frac{2}{mr_0} \left(L_1 - \frac{1}{a_0} \right), \quad (21)$$

$$g_0^{(0)} = \left(-\frac{2}{mr_0} \right)^{1/2}. \quad (22)$$

The remaining cutoff dependence in Eq. (20) can be made arbitrarily small by taking the cutoff arbitrarily large. For a cutoff $\Lambda \gtrsim M_{hi}$, those terms are no larger than higher-order terms. We are free to neglect this residual cutoff dependence at LO, as it will be removed by LECs appearing at higher orders. What we have done here is to carry out the procedure of Ref. [7] in the s wave. Equation (20) has the form of the effective-range expansion truncated at the level of the effective range. The parameters a_0 and r_0 are nothing but the standard scattering length and effective range, respectively. They are obtained by fitting the underlying or empirical amplitude at two momenta. With the assumed scalings (10) and (17), they are both large in the sense that they are set by the low-energy scale, $|a_0| \sim |r_0| = \mathcal{O}(1/M_{lo})$. While Eq. (21) allows for any sign of a_0 , Eq. (22) requires $r_0 < 0$.

The same LO amplitude was obtained in a formulation without the dimer field where the no- and two-derivative contact interactions have a different scaling than here, which demands their resummation [15]. Renormalization could only be implemented for $r_0 < 0$. The resulting pole structure was discussed in detail. In particular, $r_0 < 0$ constrains resonance poles to be in the lower half of the complex momentum plane with

$$k_I^{(0)} = -\frac{1}{r_0} > 0, \quad (23)$$

$$k_R^{(0)} = -\frac{1}{r_0} \sqrt{\frac{2r_0}{a_0} - 1} > 0, \quad (24)$$

for $2r_0 < a_0 < 0$. In the limit $\Lambda \rightarrow \infty$, Eq. (20) can be rewritten as Eq. (8) with

$$\phi^{(0)}(E) = 0. \quad (25)$$

From the assumed PC, $k_I^{(0)} \sim k_R^{(0)} = \mathcal{O}(M_{lo})$, or alternatively $\Gamma^{(0)} \sim E_R^{(0)} = \mathcal{O}(M_{lo}^2/m)$.

Resonance pole positions in the lower half-plane are in agreement with the general requirement on the S matrix [18, 24, 25] that leads to states decaying with time. The constraint $r_0 < 0$ in Eq. (20) allows also for two purely imaginary poles, one of which is a virtual state on the negative imaginary axis and the other, either a virtual state (for $a_0 < 2r_0$) or a bound state on the positive imaginary axis (for $a_0 > 0$) [15]. Other possibilities, thought to be unphysical, are excluded by renormalization.

Here, the pole location constraint arises from the standard, positive sign of the kinetic term of the dimer in the Lagrangian (1). At the two-body level there seems to be no *a priori* restriction on the sign of the dimer kinetic term [9, 26]. When this kinetic term is treated perturbatively, as is the case when there is a single low-energy pole (bound or virtual state), either sign seems to be allowed in many-body calculations [1]. The dimer in this situation involves no correlation among the four-field interactions of a no-dimer formulation. When the kinetic term is treated nonperturbatively for a positive effective range, however, the additional two-body pole leads to problems in the solution of the three-body system [27] and presumably higher-body systems as well.

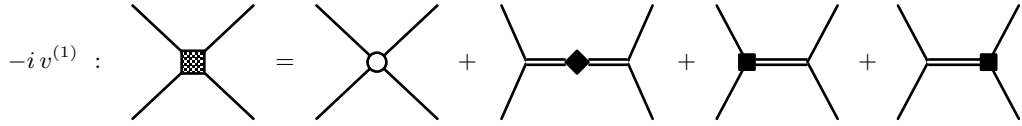


FIG. 2: Next-to-leading-order potential from the four-particle contact interaction (empty circle), dimer residual mass (solid diamond), and two-particle/dimer coupling (solid square). Other symbols as in Fig. 1.

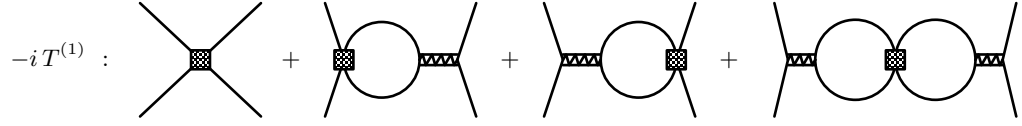


FIG. 3: Next-to-leading-order T matrix for a broad resonance in terms of the NLO potential (shaded square, Fig. 2) and the LO T matrix (shaded double line, Fig. 1).

The remainder of the inverse of the LO T matrix,

$$\delta T^{(1)-1}(k) \equiv \frac{m}{4\pi} (L_{-1} k^2 + \dots), \quad (26)$$

indicates that corrections enter at NLO, with $g_0^{(1)}$ adjusted to keep the effective range unchanged. However, $g_0^{(1)}$ induces cutoff dependence in the scattering length, which can be corrected with $\Delta^{(1)}$. This leads to the scaling

$$g_0^{(1)} = \mathcal{O}\left(\frac{M_{lo}}{M_{hi}} \sqrt{\frac{M_{lo}}{m}}\right), \quad \Delta^{(1)} = \mathcal{O}\left(\frac{M_{lo}^3}{m M_{hi}}\right). \quad (27)$$

NDA implies $C_0^{(1)}$, Eq. (19), enters at this order as well.

These contributions add to a correction in the energy-dependent potential, displayed in Fig. 2. The NLO potential is then inserted once in diagrams with LO interactions as sketched in Fig. 3. A more explicit drawing of the corresponding diagrams can be found in Fig. 4. This procedure, also known as first-order distorted-wave perturbation theory, leads to

$$\begin{aligned} \frac{4\pi}{m} \left(\frac{T^{(1)}}{T^{(0)2}} - \delta T^{(1)-1} \right) &= C_0^{(1)} \left(L_1 - \frac{1}{a_0} \right)^2 - g_0^{(1)} \left(L_1 - \frac{1}{a_0} \right) \sqrt{-2mr_0} - \Delta^{(1)} \frac{mr_0}{2} \\ &\quad + \left[C_0^{(1)} \left(L_1 - \frac{1}{a_0} \right) - g_0^{(1)} \sqrt{-\frac{mr_0}{2}} - \frac{L_{-1}}{r_0} \right] r_0 k^2 + C_0^{(1)} \frac{r_0^2 k^4}{4} - L_{-3} k^4 + \dots \\ &= -P_0 \left(\frac{r_0}{2} \right)^3 k^4 + \dots \end{aligned} \quad (28)$$

The four-particle contact interaction $C_0^{(1)}$ introduces a k^4 dependence, which leads to a non-vanishing shape parameter $|P_0| = \mathcal{O}(M_{lo}/M_{hi})$. This additional parameter at NLO requires fitting the underlying or empirical amplitude at an additional momentum. At the same time, the linear cutoff-dependence in L_1 appears in the other two terms in Eq. (28), which means that in addition to $C_0^{(1)}$ we indeed need both $\Delta^{(1)}$ and $g_0^{(1)}$ for renormalization. In Eq. (28) we imposed that the LO renormalized parameters a_0 and r_0 were not changed, leading to the running of $\Delta^{(1)}$ and $g_0^{(1)}$:

$$C_0^{(1)} = -\frac{r_0 P_0}{2}, \quad (29)$$

$$g_0^{(1)}(\Lambda) = -\left(-\frac{2}{mr_0}\right)^{1/2} \left[\frac{r_0 P_0}{2} \left(L_1 - \frac{1}{a_0} \right) + \frac{L_{-1}}{r_0} \right], \quad (30)$$

$$\Delta^{(1)}(\Lambda) = \frac{2}{mr_0} \left(L_1 - \frac{1}{a_0} \right) \left[\frac{r_0 P_0}{2} \left(L_1 - \frac{1}{a_0} \right) + \frac{2L_{-1}}{r_0} \right]. \quad (31)$$

Again $g_0^{(1)}(\Lambda)$ is real due to the constraint $r_0 < 0$ stemming from a positive dimer kinetic term.

The amplitude up to NLO can be written as

$$T^{(0+1)}(k) = -\frac{4\pi}{m} \left[-\frac{1}{a_0} + \frac{r_0}{2} k^2 - P_0 \left(\frac{r_0}{2} \right)^3 k^4 - ik \right]^{-1} + \dots \quad (32)$$

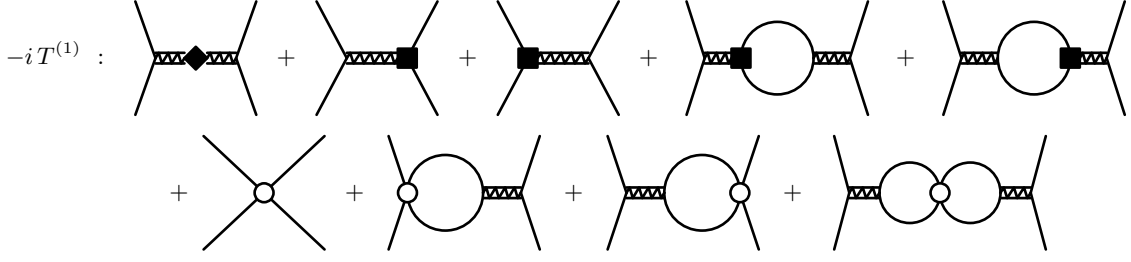


FIG. 4: Extended version of the next-to-leading-order T matrix for a broad resonance in Fig. 3. Notation as in Figs. 1 and 2.

Again, this amplitude was obtained from momentum-dependent interactions in Ref. [15]. The NLO correction (28) is perturbative within the regime of applicability of the EFT, so it does not lead to new poles. Our choice of keeping LO renormalized parameters unchanged does mean the poles are slightly displaced from their LO positions, as discussed in Ref. [15]:

$$k_I^{(0+1)} = -\frac{1}{r_0} \left[1 + P_0 \left(\frac{r_0}{a_0} - 1 \right) \right] > 0, \quad (33)$$

$$k_R^{(0+1)} = -\frac{1}{r_0} \sqrt{\frac{2r_0}{a_0} - 1} \left[1 + P_0 \left(1 - \frac{r_0^2/2a_0^2}{2r_0/a_0 - 1} \right) \right] > 0. \quad (34)$$

The NLO correction amounts to a background [18, 28] proportional to P_0 : again up to higher-order terms, the S matrix can be written as Eq. (8) with [15]

$$\phi^{(0+1)}(E) = \frac{P_0 r_0}{2} \sqrt{mE}. \quad (35)$$

The “...” in Eq. (32) contain terms $\propto \Lambda^{-3}$ indicating that new interactions appear at or before $N^3\text{LO}$. For example, from NDA we expect g_2 and C_2 to appear at $N^2\text{LO}$ and $N^3\text{LO}$, respectively. These corrections can be incorporated following the procedure described above, although expressions become lengthier as we have to consider multiple insertions of subleading interactions — for example, two insertions of NLO interactions at $N^2\text{LO}$. We refrain from this exercise here, shifting instead to a qualitatively different case.

IV. NARROW RESONANCE

A narrow resonance is one for which $\Gamma \ll E_R$, or equivalently $k_I \ll k_R$. In this case the quantum corrections to the bare dimer propagator are generically small. In zeroth order in perturbation theory, the poles lie on the real axis, with the ik from Eq. (12) a correction to Eq. (11) that requires no resummation, except in a small window of energies around the resonance [8]. In Sec. IV A we consider generically low momenta, while the region around the resonance is tackled in Sec. IV B.

A. Generic momenta

We can account for a narrow resonance by adjusting the PC of the previous section. Since the contribution from loop integrals does not change, we need a new scaling for $g_0^{(0)}$ [8],

$$g_0^{(0)} = \mathcal{O} \left(\sqrt{\frac{M_{lo}^2}{m M_{hi}}} \right). \quad (36)$$

Each loop comes with a factor of Q/M_{hi} and is therefore perturbative for generic momenta $Q \sim M_{lo}$. A side effect of the smallness of $g_0^{(0)}$ is that a natural C_0 ,

$$C_0^{(0)} = \mathcal{O} \left(\frac{1}{M_{hi}} \right), \quad (37)$$

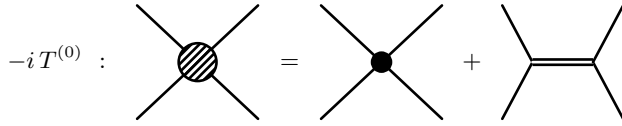


FIG. 5: Leading-order T matrix in the presence of a narrow resonance for generic momenta, in terms of the leading four-particle contact interaction (filled circle) and the bare dimer propagator (double line).

now appears at LO [13].

The LO T matrix now is simply the sum of tree-level diagrams — the bare dimer propagator (11) and the four-particle contact interaction — shown in Fig. 5. That is,

$$T^{(0)}(k) = \frac{4\pi}{m} \left(C_0^{(0)} + g_0^{(0)2} D_0^{(0)}(k) \right) = \frac{4\pi}{m} a_0 \frac{k^2/k_0^2 - 1}{k^2/k_r^2 - 1}, \quad (38)$$

where we defined

$$\Delta^{(0)} = \frac{k_r^2}{m}, \quad (39)$$

$$g_0^{(0)} = \left[a_0 \left(\frac{k_r^2}{k_0^2} - 1 \right) \frac{k_r^2}{m} \right]^{1/2}, \quad (40)$$

$$C_0^{(0)} = \frac{k_r^2}{k_0^2} a_0. \quad (41)$$

The amplitude (38) has real poles,

$$k_I^{(0)} = 0, \quad (42)$$

$$k_R^{(0)} = k_r > 0, \quad (43)$$

with $k_r = \mathcal{O}(M_{lo})$, for $\Delta^{(0)} > 0$. ($\Delta^{(0)} < 0$, on the other hand, generates a bound/virtual state pair. We do not consider this case explicitly, although there is no obvious obstacle to do so.) As we discuss in detail in Sec. IV B, corrections to Eq. (38) are large in the immediate neighborhood of these poles. In addition, the presence of $C_0^{(0)}$ at LO together with the dimer field leads to amplitude zeros at $k = \pm k_0$, $|k_0| = \mathcal{O}(M_{lo})$. For $\Delta^{(0)} > g_0^{(0)2}/C_0^{(0)}$, a zero $k_0 > 0$ occurs on the scattering axis. In the particular case $k_0 = 0$ — that is, $g_0^{(0)2} = C_0^{(0)} \Delta^{(0)}$ — the T matrix vanishes at threshold, which means that the scattering length $a_0 = 0$. More generally, $|a_0| = \mathcal{O}(1/M_{hi})$ but the sign of a_0 is constrained by the relative sizes of k_r^2 and k_0^2 ,

$$a_0 k_r^2 \left(\frac{k_r^2}{k_0^2} - 1 \right) > 0, \quad (44)$$

so that $g_0^{(0)}$ in Eq. (40) is real.

The dimer part of the T matrix (38) was put forward in Ref. [8]. Reference [13] was the first to point out that C_0 should be included as well on the basis of NDA, but its role in producing an amplitude zero was not mentioned. In contrast to the case of a broad resonance, in general three non-vanishing parameters need to be determined at LO, which requires data at three different momenta. One can be taken as the location k_0 of the T -matrix zero. The positions of the poles will be displaced at NLO and only their real part k_R can be used as input at LO. As a third input we can take, for example, the amplitude at $k = 0$, that is, the scattering length a_0 .

For the present case there is no residual cutoff dependence at LO and no need for new interactions at NLO. However, the one-loop diagrams will bring in cutoff dependence, requiring for renormalization NLO shifts in the three LECs already present at LO:

$$g_0^{(1)} = \mathcal{O} \left(\frac{M_{lo}}{M_{hi}} \sqrt{\frac{M_{lo}^2}{m M_{hi}}} \right), \quad \Delta^{(1)} = \mathcal{O} \left(\frac{M_{lo}^3}{m M_{hi}} \right), \quad C_0^{(1)} = \mathcal{O} \left(\frac{M_{lo}}{M_{hi}^2} \right). \quad (45)$$

Like for a broad resonance, these corrections add to the energy-dependent potential of Fig. 2, which however must be included here in first order of simple, non-distorted perturbation theory along with the one-loop diagrams involving

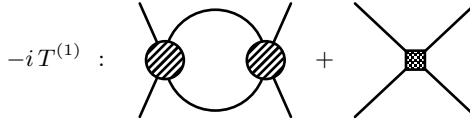


FIG. 6: Next-to-leading-order T matrix for generic momenta in the presence of a narrow resonance, in terms of the one-loop correction to LO T matrix (hatched blob, Fig. 5) and the NLO potential (shaded square, Fig. 2).

LO LECs. The diagrams in Fig. 6 amount to

$$\frac{4\pi}{m} \frac{T^{(1)}}{T^{(0)2}} = \frac{C_0^{(1)} + 2g_0^{(0)} g_0^{(1)} D_0^{(0)} + g_0^{(0)2} \Delta^{(1)} D_0^{(0)2}}{(C_0^{(0)} + g_0^{(0)2} D_0^{(0)})^2} - L_1 - ik - L_{-1} k^2 + \dots \quad (46)$$

The cutoff dependence from L_1 can be absorbed in the NLO bare parameters,

$$\Delta^{(1)}(\Lambda) = a_0 \left(\frac{k_r^2}{k_0^2} - 1 \right) \frac{k_r^2}{m} L_1, \quad (47)$$

$$g_0^{(1)}(\Lambda) = -a_0 \frac{k_r^2}{k_0^2} \left[a_0 \left(\frac{k_r^2}{k_0^2} - 1 \right) \frac{k_r^2}{m} \right]^{1/2} L_1, \quad (48)$$

$$C_0^{(1)}(\Lambda) = \left(a_0 \frac{k_r^2}{k_0^2} \right)^2 L_1, \quad (49)$$

in order to keep the physical parameters that appear at LO unchanged. Up to higher-order terms, the amplitude including NLO corrections is then

$$T^{(0+1)}(k) = \frac{4\pi}{m} \left(\frac{1}{a_0} \frac{k^2/k_r^2 - 1}{k^2/k_0^2 - 1} + ik + L_{-1} k^2 + \dots \right)^{-1}, \quad (50)$$

with residual cutoff dependence $\propto \Lambda^{-1}$. After renormalization the only effect of NLO is to introduce the parameter-free unitarity term ik . Since $|a_0^{-1}| = \mathcal{O}(M_{hi})$, this term is indeed relatively small by $\mathcal{O}(M_{lo}/M_{hi})$ for $Q = \mathcal{O}(M_{lo})$. The number of LECs at LO and NLO are the same and there is no need of more data input at NLO. Expanding the denominator of Eq. (50) in powers of k/k_0 we can relate it to the effective-range expansion. For example, the effective range is

$$r_0 = -\frac{2}{a_0 k_r^2} \left(\frac{k_r^2}{k_0^2} - 1 \right) < 0, \quad (51)$$

considering the constraint (44). Just as for a broad resonance, we recover the well-known constraint on the effective range from the non-ghost character of the dimer. In contrast to a broad resonance, however, here $|r_0| = \mathcal{O}(M_{hi}/M_{lo}^2)$ is large, with $|a_0/r_0| = \mathcal{O}(M_{lo}^2/M_{hi}^2)$. This is a feature of an amplitude with a low-energy zero [5]. Examples where an s -wave zero is important are low-energy nucleon-nucleon [29] and nucleon-deuteron [30] scattering in, respectively, 1S_0 and $^2S_{1/2}$ channels, but both appear together with virtual states instead of resonances.

The amplitude (50) is, however, not equivalent to the effective-range expansion truncated at the effective-range term, as is the case for a broad resonance (see Eq. (20) and Ref. [15]). In addition to the effective range, we obtain a string of higher powers of k^2 in the denominator of Eq. (50) which are suppressed with respect to the effective-range term by only $\mathcal{O}(Q^2/M_{lo}^2)$. These powers, of course, resum into an amplitude zero. In order to obtain Eq. (20) from Eq. (50) we need an additional fine tuning to enhance g_0 .

A visible effect of the unitarity term is to displace the real poles of the LO amplitude (38) in the imaginary direction. The fine tuning embodied in our PC results in a small imaginary part k_I compared to the real part, $k_I/k_R = \mathcal{O}(M_{lo}/M_{hi})$:

$$k_I^{(0+1)} = \frac{a_0 k_r^2}{2} \left(\frac{k_r^2}{k_0^2} - 1 \right) > 0, \quad (52)$$

$$k_R^{(0+1)} = k_r > 0. \quad (53)$$

Also for a narrow resonance the location of the resonance pole in the lower half-plane goes hand-in-hand with a negative effective range, Eq. (51).

The residual cutoff dependence in Eq. (50) indicates that further corrections appear at N^2LO term. Again, proceeding to higher orders is straightforward but tedious. They will not change the qualitatively important features of LO and NLO.

B. Small window around the resonance

From the NLO amplitude (50) for generically low momenta we see the emergence of a narrow pole with $k_I = \mathcal{O}(M_{lo}^2/M_{hi}) \ll k_R = \mathcal{O}(M_{lo})$ or, alternatively, $\Gamma = \mathcal{O}(M_{lo}^3/mM_{hi}) \ll E_R = \mathcal{O}(M_{lo}^2/m)$. Unfortunately the expansion of the T matrix obtained in the preceding subsection does not converge sufficiently close to the pole [8]. As k approaches k_R , the LO amplitude (38) grows way beyond the $\mathcal{O}(4\pi/mM_{hi})$ magnitude it has for a generic $k = \mathcal{O}(M_{lo})$, and in fact diverges at $k = k_r$. The first quantum correction to the bare dimer propagator diverges twice as fast, and more loops insertions even faster. The series stops converging in a window $|k - k_R| \sim k_I$ around the resonance, or in terms of energy, $|E - E_R| \sim \Gamma$. (Note that on account of Eq. (52) the window size is limited by the presence of the zero, and if the zero is fine-tuned close to the resonance the window can be made even narrower.)

With $g_0^{(0)}$ scaling as in Eq. (36) we have, within this window around the resonance,

$$\left. \frac{D_1(k)}{D_0^{(0)}(k)} \right|_{\text{window}} = \mathcal{O} \left(\frac{mg_0^{(0)2} M_{hi}}{M_{lo}^2} \right) = \mathcal{O}(1) , \quad (54)$$

instead of Eq. (15). In contrast to a broad resonance, here a resummation of the dimer propagator is necessary as a consequence of a kinematical fine tuning. The dressed propagator is now larger than $C_0^{(0)}$ by a factor of $\mathcal{O}(M_{hi}/M_{lo})$. Despite the weakness of $g_0^{(0)}$ compared to the broad resonance case, the LO T matrix is given by the full dimer propagator in Fig. 1 and requires renormalization of the residual mass for which the $\Delta^{(0)}(\Lambda)$ in Eq. (39) is insufficient. The LO T matrix in the window has the same form as Eq. (20) [8, 13, 14] and can be written as

$$T^{(-1)}(k) \Big|_{\text{window}} = \frac{4\pi}{m} g_0^{(0)2} D^{(0)}(k) = \frac{4\pi}{m} \left[\frac{1}{2k_I} (k^2 - k_R^2) + ik + L_{-1} k^2 + \dots \right]^{-1} , \quad (55)$$

where, keeping the notation of the previous subsection,

$$\Delta^{(0)}(\Lambda) + \Delta^{(1)}(\Lambda) = \frac{1}{m} (k_R^2 + 2k_I L_1) , \quad (56)$$

$$g_0^{(0)} = \left(\frac{2k_I}{m} \right)^{1/2} . \quad (57)$$

Apart from higher-order terms, the S matrix is again given by Eq. (8) with no background,

$$\phi^{(-1)}(E) = 0 . \quad (58)$$

Like for a broad resonance, it contains two parameters but the relations between pole parameters $k_{R,I}$ and effective range parameters in Eqs. (23) and (24) no longer hold.

The NLO amplitude now receives contributions from $C_0^{(0)}$ (instead of $C_0^{(1)}$) as well as corrections to the two-particle dimer vertex and the dimer residual mass needed for renormalization. The NLO potential is given by Fig. 2 and the NLO T matrix, by Fig. 3 or, more explicitly, Fig. 4. These corrections were first considered in Ref. [13], where only the first diagram in the second line of Fig. 4 was included. Reference [14] pointed out the need for additional loop diagrams, and included the second and third diagrams in the second line of Fig. 4. However, the last diagram in Fig. 4 was omitted even though it is of the same order. Including all diagrams,

$$T^{(-1+0)}(k) \Big|_{\text{window}} = \frac{4\pi}{m} \left[\frac{2k_I}{k^2 - k_R^2 + 2ik_I k} \left(1 + \frac{2k_I^2}{k^2 - k_R^2 + 2ik_I k} \right) + c \left(1 - \frac{4ik_I k}{k^2 - k_R^2 + 2ik_I k} \right) \right] \quad (59)$$

$$= \frac{4\pi}{m} \left\{ \frac{1}{2k_I} (k^2 - k_R^2 - k_I^2) + ik - c \left[\frac{(k^2 - k_R^2)^2}{4k_I^2} + k^2 \right] + \dots \right\}^{-1} , \quad (60)$$

if we set

$$C_0^{(0)} = c , \quad (61)$$

$$g_0^{(1)}(\Lambda) + g_0^{(2)}(\Lambda) = - \left(\frac{2k_I}{m} \right)^{1/2} [c(L_1 + k_I) + k_I L_{-1}] , \quad (62)$$

$$\Delta^{(2)}(\Lambda) = \frac{k_I}{m} \left\{ 2c \left[(L_1 + k_I)^2 + k_R^2 - k_I^2 \right] + k_I + 2L_{-1} (2k_I L_1 + k_R^2) \right\} , \quad (63)$$

with c a constant. The cutoff-independent terms in the expressions above were chosen so that the pole positions do not change and there is no double pole at NLO, except for the k_I^2 correction in Eq. (59), which accounts for the k_I^2 in Eq. (7). As a consequence, the S matrix just acquires a background phase

$$\phi^{(-1+0)}(E) = -c \sqrt{mE}. \quad (64)$$

Equation (59) agrees with the corresponding result in Ref. [14] despite the missing diagram in the latter. This diagram brings in both a momentum-independent quadratic divergence L_1^2 and a linear divergence L_1 proportional to ik , in addition to a finite term proportional to k^2 that contributes to the renormalization of $g_0^{(2)}$. The quadratic divergence is absorbed in $\Delta^{(2)}$, Eq. (63), together with a (momentum-independent) linear divergence L_1 from other diagrams and the residual cutoff dependence L_{-1} from LO diagrams. The linear divergence proportional to ik from the missing diagram, being non-analytic in energy, cannot be absorbed anywhere, but it cancels an opposite linear divergence from other diagrams. Other diagrams also induce additional cutoff dependence of types L_1 and L_{-1} , which are absorbed in $g_0^{(1)} + g_0^{(2)}$, Eq. (62). Two combination of LECs are necessary and sufficient to remove the cutoff dependence from an arbitrary regulator. The cancellation in the non-analytic linearly divergent terms is absent in the incomplete set of diagrams considered in Ref. [14]. But the error was inconsequential because Ref. [14] used dimensional regularization with minimal subtraction, which makes $L_1 = 0 = L_{-1}$. In this particular case not only does the missed diagram cause no problem, but also no shifts in g_0 and Δ are needed explicitly. In general, however, only the inclusion of all diagrams of a given order — here, all diagrams in Fig. 4 — leads to a renormalized result. Reference [14] also looked into N^2LO corrections, but again many diagrams are missing, such as the analog of the last diagram in Fig. 4 with an additional loop and C_0 vertex in the middle. The additional diagrams can be included straightforwardly and renormalization performed following the procedure we presented above.

So far in this subsection we have written the amplitude in terms of parameters like k_R , k_I , and c that are in principle determined from data within the resonance window. For simplicity, we kept the same notation for some parameters as in the previous subsection, with the implication that Eqs. (53), (52), and (41) hold. To see that that is indeed the case, we rewrite Eq. (60) with only a higher-order error as

$$\left(\frac{m}{4\pi} T^{(-1+0)}(k)\right)^{-1}_{\text{window}} = \underbrace{\frac{1}{c} \frac{k^2 - k_R^2}{k^2 - (k_R^2 - 2k_I/c)} + ik}_{\mathcal{O}(M_{lo})} \underbrace{- \frac{k_I}{2} - ck^2}_{\mathcal{O}\left(\frac{M_{lo}^2}{M_{hi}}\right)} + \dots. \quad (65)$$

To relate the parameters around the resonance to those outside the resonance window we match this expression to Eq. (50),

$$\left(\frac{m}{4\pi} T^{(0+1)}(k)\right)^{-1} = \underbrace{\frac{k_0^2}{a_0 k_r^2} \frac{k^2 - k_r^2}{k^2 - k_0^2}}_{\mathcal{O}(M_{hi})} \underbrace{+ ik}_{\mathcal{O}(M_{lo})} + \dots. \quad (66)$$

At the first common order, $\mathcal{O}(M_{lo})$,

$$k_R = k_r > 0, \quad (67)$$

$$k_I = \frac{a_0 k_r^2}{2} \left(\frac{k_r^2}{k_0^2} - 1 \right) > 0, \quad (68)$$

$$c = a_0 \frac{k_r^2}{k_0^2}, \quad (69)$$

in agreement with Eqs. (53), (52), and (41). These relations plus their analogs at higher orders ensure the consistency of the T matrix in the two regions, inside and outside of the resonance window.

V. TOY MODEL

One of the important features of an EFT is its model independence, which means the EFT describes the low-energy limit of different underlying theories as long as the separation of scales in all of them follows the same pattern. The details of the underlying dynamics are encoded in the renormalized values of the LECs, the relative importance of which is captured by PC. Here we exemplify the systematic character of the resulting expansions for observables, taking a particular potential model as an underlying theory.

The toy model we use comprises an attractive spherical well of range R and depth β^2/mR^2 with a repulsive delta shell with strength α/mR at its edge:

$$V(r) = \frac{\alpha}{mR} \delta(r - R) - \frac{\beta^2}{mR^2} \theta(R - r), \quad (70)$$

with $\alpha > 0$ and $\beta > 0$. In Ref. [15] this model was used to illustrate the EFT expansion for a broad resonance, which was reproduced in Sec. III using a dimer field. The same model had been considered in Ref. [13] to inform the scalings of various LECs near a narrow resonance. We revisit the model in the context of Sec. IV, confirming the presence of the amplitude zero and providing an explicit example of convergence for low-energy observables.

A. Phase shift and poles

For the s wave, the phase shift can be obtained easily,

$$\cot \delta_0(k) = -\frac{(\sqrt{k^2 R^2 + \beta^2} \cot \sqrt{k^2 R^2 + \beta^2} + \alpha) \cot(kR) + kR}{\sqrt{k^2 R^2 + \beta^2} \cot \sqrt{k^2 R^2 + \beta^2} + \alpha - kR \cot(kR)}. \quad (71)$$

We are interested in the low-energy region, $|k| \ll R^{-1}$. If we expand this expression in powers of kR , the very low-energy tail is given by the effective-range expansion. Expressions and plots for the scattering length a_0 and the effective range r_0 can be found, for example, in Ref. [15].

The model yields resonances and amplitude zeros. A resonance appears when $\cot \delta_0(k_{\pm}) - i = 0$ for complex momenta k_{\pm} , which translates to

$$\sqrt{k_{\pm}^2 R^2 + \beta^2} \cot \sqrt{k_{\pm}^2 R^2 + \beta^2} = -\alpha + ik_{\pm} R. \quad (72)$$

In contrast, a real zero arises from $\cot \delta_0(k_0) \rightarrow \pm\infty$, or

$$\sqrt{k_0^2 R^2 + \beta^2} \cot \sqrt{k_0^2 R^2 + \beta^2} = -\alpha + k_0 R \cot(k_0 R). \quad (73)$$

As pointed out in Ref. [13], we expect the resonance to be narrow when the strength of the delta-shell potential is large, $\alpha \gg 1$. In this case, one can solve Eqs. (72) and (73) as expansions in α^{-1} . One finds a sequence of resonances labeled by a positive integer $n = 1, 2, \dots$,

$$k_{Rn} R = n\pi \left[1 - \left(\frac{\beta}{n\pi} \right)^2 - \frac{2}{\alpha} + \frac{3}{\alpha^2} + \frac{2}{3\alpha^3} (n^2\pi^2 - 6) + \mathcal{O}(\alpha^{-4}) \right]^{1/2}, \quad (74)$$

$$k_{In} R = \frac{(n\pi)^2}{\alpha^2} \left[1 - \frac{3}{\alpha} + \mathcal{O}(\alpha^{-2}) \right]. \quad (75)$$

Each narrow resonance is accompanied by a zero of the amplitude below it,

$$(k_{0n} R)^2 = (k_{Rn} R)^2 - 2 \left(\frac{n\pi}{\alpha} \right)^2 [1 + \mathcal{O}(\alpha^{-1})]. \quad (76)$$

For specific values of α and β , a resonance exists within the low-energy region. For the lowest narrow resonance to be in the low-energy region,

$$\frac{\pi}{\alpha} \ll 1, \quad \pi^2 - \beta^2 - \frac{2\pi^2}{\alpha} \ll 1. \quad (77)$$

As a concrete case, we take

$$\alpha = 2\pi^2, \quad \beta^2 = \pi^2 - 1. \quad (78)$$

The corresponding phase shift is shown in Fig. 7. The left panel displays $kR \cot \delta_0(k)$ as a function of kR . At very small energy, the curve is approximately quadratic with

$$\frac{a_0}{R} \simeq 0.40329, \quad \frac{r_0}{R} \simeq -86.04272. \quad (79)$$

As the energy increases, the divergence associated with the amplitude zero becomes clearly visible at $k_0 R \simeq 0.2$. As the energy increases just a bit further, $\cot \delta_0(k)$ vanishes at $k_r R \simeq 0.3$. This is the resonance region, where a narrow resonance manifests itself as a peak in the cross section $\sigma_0 \propto \sin^2 \delta_0(k)$. On the right panel, the peak around $k_r R \simeq 0.3$ is seen in the plot of $\sin^2 \delta_0(k)$ as a function of kR . The values for the pole and zero momenta, k_{\pm} and k_0 , are listed in Table I.

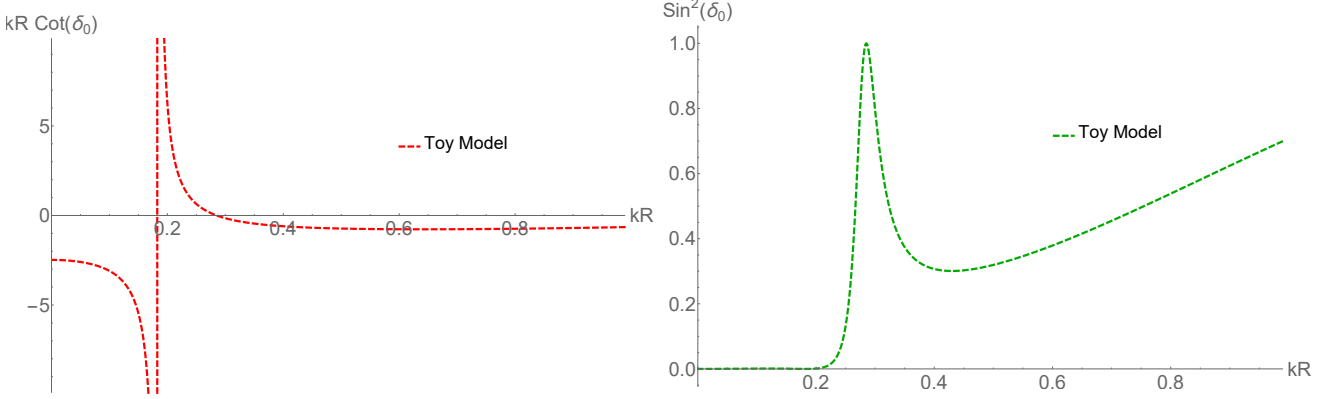


FIG. 7: s -wave phase shift for the potential (70) with α and β in Eq. (78), as function of the momentum in units of the inverse range (R^{-1}): $kR \cot \delta_0$ (left panel) and $\sin^2 \delta_0$ (right panel).

	$k_R R$	$k_I R$	$k_0 R$
LO EFT	0.281 ± 0.022	0.000 ± 0.022	0.18265
NLO EFT	0.281 ± 0.004	0.022 ± 0.004	0.18265
Toy model	0.278159	0.021427	0.18265

TABLE I: Positions of the resonance poles ($k_{R,I}$) and the zero of the T matrix (k_0) in units of the inverse interaction range (R^{-1}). The EFT at LO and NLO is compared with the potential (70) with α and β in Eq. (78).

B. Comparison with EFT

We now describe this physics with the EFT of Sec. IV. The toy-model parameter choice (78) gives $k_I/k_R = 1/2\sqrt{3}\pi \simeq 1/11$ through Eqs. (74) and (75). Since $k_I/k_R = \mathcal{O}(M_{lo}/M_{hi})$ in our PC, we identify the expansion parameter as $M_{lo}/M_{hi} \sim 1/10$. Our PC indeed captures within factors of 2 or 3 the magnitude of the various quantities calculated in the toy model:

- $a_0/R = \mathcal{O}(1)$ and $|r_0|/R = \mathcal{O}(M_{hi}^2/M_{lo}^2)$ in Eq. (79);
- $k_0 R = \mathcal{O}(M_{lo}/M_{hi})$ in Table I;
- $k_r R = \mathcal{O}(M_{lo}/M_{hi})$, related to a_0 , r_0 , and k_0 by Eq. (51).

The EFT amplitude at LO for generic low momenta, Eq. (38), has three parameters, which we choose to fit to the position of the amplitude zero in Table I and to the effective-range parameters in Eq. (79). At NLO the phase shift does not change because the form of $k \cot \delta_0(k)$ in Eq. (50) is the same as in LO. The corresponding error can be estimated from the residual cutoff dependence in $k \cot \delta_0(k)$ as $\pm \theta_{-1} k^2 R^{-1}$. The EFT phase shift, $\delta_0(k)$, is compared to the toy-model phase shift on the left panel of Fig. 8. We see that, despite all fit parameters being determined at momenta at or below k_0 , the NLO EFT reproduces the toy model within error bars throughout the low-energy region.

Although the phase shift (and thus the zero position) is the same at LO and NLO, the pole positions change at NLO due to the unitary term. At LO the resonance pole is on the real axis, Eqs. (42) and (43). The LO T matrix in Eq. (38) does not contain any residual cutoff dependence which could be used to estimate the error in the LO pole position. This error is $\mathcal{O}(M_{lo}/M_{hi})$ and could be expressed in a number of ways in terms of the parameters appearing in Eq. (38). One possible combination is taking the average of k_0 and k_r as representative of M_{lo} , and a_0 as representative of M_{hi} , leading to an error of magnitude

$$|\Delta(k_{\pm}^{(0)} R)| = \frac{a_0}{R} \left(\frac{k_r R + k_0 R}{2} \right)^2. \quad (80)$$

At NLO, the resonance poles move below the real axis according to Eqs. (52) and (53). We can translate the error from the residual cutoff dependence into

$$|\Delta(k_{\pm}^{(1)} R)| = \frac{a_0}{\pi R} (k_r R)^3 \left[\frac{(k_r R)^2}{(k_0 R)^2} - 1 \right]. \quad (81)$$

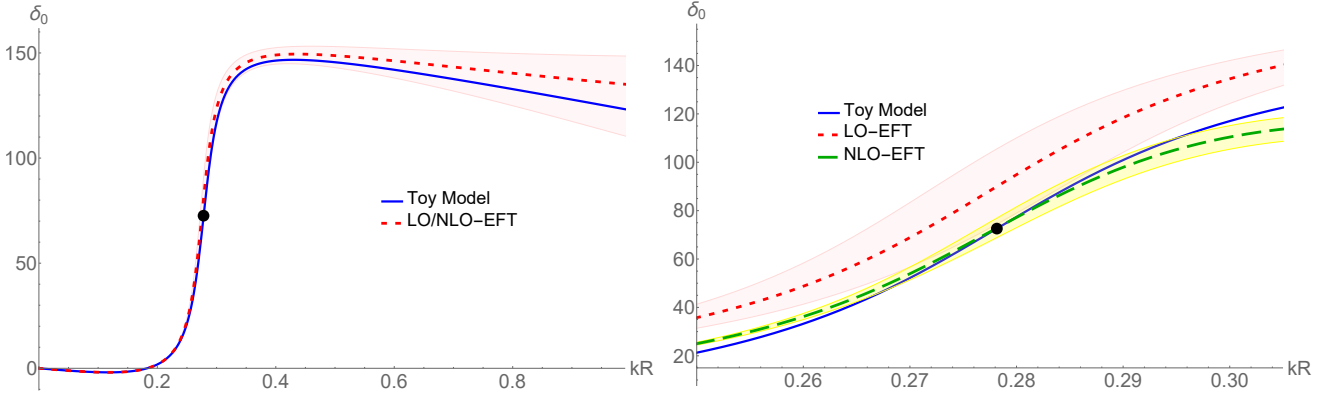


FIG. 8: s -wave phase shift δ_0 in the EFT at LO and NLO as function of the momentum in units of the inverse range (R^{-1}) compared to the result (solid blue line) from the potential (70) with α and β in Eq. (78). Left panel: LO/NLO phase shift (red dashed line) and error (red shadow band) obtained from Eqs. (38) and (50). Right panel: LO phase shift (red dotted line) and error (red shadow band), and NLO phase shift (green dashed line) and error (yellow shadow band) from Eqs. (55) and (60), respectively, in a small window around the narrow resonance. The value of the real part of the resonance momentum is marked by a black dot on the blue line.

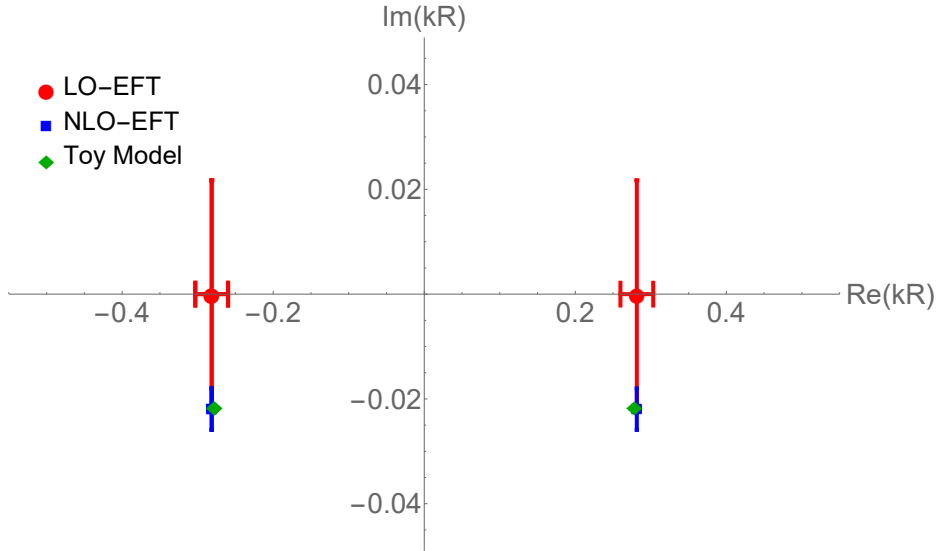


FIG. 9: Pole positions in the EFT at LO (red circle and error bars) and NLO (blue square and error bars) compared to the result (green diamond) from the potential (70) with α and β in Eq. (78).

The EFT approximation for the pole positions is given in Table I and represented graphically in Fig. 9. As we can see, LO and NLO results include the toy-model poles within their respective errors. Both central values and errors are converging systematically, confirming that the EFT is working properly.

Within a small window around the narrow resonance, the changes in pole positions are relatively large. An estimate of the size of the window is given by the magnitude of the imaginary part of the pole momentum, *i.e.* $|k - k_R|R \sim k_I R \simeq 0.02$ around k_R . Resummation of the quantum corrections that produce the resonance width leads to the LO amplitude (55), which contains two parameters, k_R and k_I . We fit them to the values from the toy model in Table I. At NLO, Eq. (60) has an additional parameter, c , which could be fitted to the phase shift at a particular momentum within the window. Alternatively, we use the matching Eqs. (67), (68), and (69) to express

$$\frac{c}{R} = \frac{2k_I R}{k_R^2 R^2 - k_0^2 R^2} \simeq 0.973707 \quad (82)$$

from the toy-model values in Table I. As expected from our PC, $c = \mathcal{O}(M_{hi})$.

Although the pole positions are exact already at LO, the phase shift changes as we go from LO to NLO. The error at LO can be estimated from the residual cutoff dependence just as the NLO error for generic momenta. The

residual cutoff dependence at NLO, on the other hand, is $\propto \Lambda^{-3}$ and would underestimate the magnitude of N²LO corrections. Since nothing in principle prevents a k^4 term in Eq. (60), which would be suppressed by two powers of M_{hi} , we estimate the error compared to ck^2 as $\pm c^2 k^4/k_R$, using k_R and c as proxies for M_{lo} and M_{hi} , respectively. Results are shown on the right panel of Fig. 8. While LO works at the 20% level, the NLO result is very close to the toy-model phase shift. Even though we have not fitted the latter directly, using the matching (82) instead, the NLO and toy-model curves intersect at k_R . We see again the systematic improvement of the EFT as order increases.

The EFT with our PC thus describes pretty well the physics encoded in a narrow resonance and its concomitant amplitude zero, just as the PC of Sec. III does [15] for a broad resonance with no low-energy amplitude zero. Next we discuss the possibility of a low-energy amplitude zero appearing together with a broad resonance.

VI. BROAD RESONANCE WITH AN AMPLITUDE ZERO

So far we have assumed that C_0 has a magnitude compatible with NDA, with only the sizes of dimer parameters affected by the low-energy scale M_{lo} . Different scalings of g_0 , Eqs. (17) and (36), lead to broad and narrow resonances, respectively. Only for narrow resonances does the amplitude have a zero in the low-energy region. In this section we consider the possibility of the existence of an amplitude zero together with a broad resonance, when Eqs. (10) and (17) are still expected to hold. This requires an additional fine tuning that makes C_0 large,

$$C_0^{(0)} = \mathcal{O}\left(\frac{1}{M_{lo}}\right). \quad (83)$$

With the assumption (83), we must resum not only the dimer propagator as in Sec. III, but also the non-derivative contact interaction. The corresponding diagrams in Fig. 10 lead to

$$T^{(0)}(k) = \frac{4\pi}{m} \frac{C_0^{(0)} + g_0^{(0)2} D_0^{(0)}(k)}{1 + (C_0^{(0)} + g_0^{(0)2} D_0^{(0)}(k)) I_0(k)} \quad (84)$$

$$= -\frac{4\pi}{m} \left(-\frac{1}{a_0} + \frac{r_0 k^2}{2} \frac{1}{1 - k^2/k_0^2} - ik - L_{-1} k^2 + \dots \right)^{-1}, \quad (85)$$

where the three LO LECs renormalize the amplitude with

$$\Delta^{(0)}(\Lambda) = \frac{k_0^2}{m} \frac{L_1 - 1/a_0}{L_1 - 1/a_0 - r_0 k_0^2/2}, \quad (86)$$

$$g_0^{(0)}(\Lambda) = \left[-\frac{r_0 k_0^4}{2m(L_1 - 1/a_0 - r_0 k_0^2/2)^2} \right]^{1/2}, \quad (87)$$

$$C_0^{(0)}(\Lambda) = -\frac{1}{L_1 - 1/a_0 - r_0 k_0^2/2}. \quad (88)$$

The amplitude is of the same form as the NLO amplitude (50) for a narrow resonance with the replacement $k_r^2 \rightarrow k_0^2(1 + a_0 r_0 k_0^2/2)^{-1}$. However, the amplitude (85) holds throughout the low-energy region, a_0 and r_0 being identified as before with the scattering length and effective range. Again, renormalization requires $r_0 < 0$ since $k_0^4 > 0$ must be real for $g_0^{(0)}(\Lambda)$ also to be real. The amplitude-zero location k_0 can be real or imaginary, but $|k_0| = \mathcal{O}(M_{lo})$. As in the amplitude (20), $|a_0| \sim |r_0| = \mathcal{O}(1/M_{lo})$. The difference lies in the other effective-range parameters, which are determined by M_{lo} instead of M_{hi} . For example, the shape parameter at LO is [29]

$$P_0^{(0)} = -\frac{4}{r_0^2 k_0^2}. \quad (89)$$

As expected, in the limit $|k_0| \rightarrow \infty$ Eq. (85) reduces to Eq. (20). At the same time, $C_0^{(0)} \rightarrow 0$, and Eqs. (86) and (87) go into Eqs. (21) and (22), respectively.

The amplitude (84) was considered with dimensional regularization and minimal subtraction in Ref. [9], while renormalization equivalent to that above was performed in Ref. [31] starting from a sharp momentum cutoff. This amplitude is frequently invoked in discussions of Feshbach resonances — see for example Ref. [32]. In this context C_0 is usually considered a natural, small background, for which resummation is actually unnecessary. The possibility of a fine-tuned C_0 , resulting in a low-energy zero, was investigated in Ref. [29] with an eye on the two-nucleon 1S_0 channel. In Ref. [30] the interest was the motion of poles in the three-nucleon system: neutron-deuteron scattering

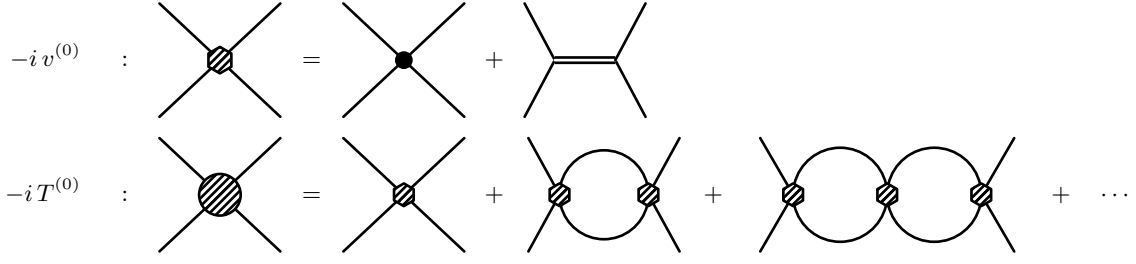


FIG. 10: Leading-order potential and T matrix for a broad resonance with an amplitude zero, in terms of the leading four-particle contact interaction (filled circle) and the dimer propagator (double line).

in the spin-3/2 channel shows a shallow amplitude zero below threshold, which moves into the scattering region as the two-nucleon system approaches unitarity. The focus of all these references was on shallow bound and/or virtual states.

Here we are interested in Eq. (85) for the description of a resonance in the presence of the zeros at $k = \pm k_0$. In order to find the poles we rearrange the denominator of the T matrix in Eq. (85) as

$$k^3 - i \frac{k^2}{a_0} \left(1 + \frac{a_0 r_0 k_0^2}{2} \right) - k k_0^2 + i \frac{k_0^2}{a_0} = 0. \quad (90)$$

For real values of a_0 , r_0 , and k_0^2 this cubic polynomial has a symmetry relative to the imaginary axis: if k is a root, so is $-k^*$. Hence the roots of Eq. (90) should either be imaginary or come in pairs symmetric with respect to the imaginary axis. Since we have only three roots there are only two possibilities: *i*) all the three roots are imaginary [29]; *ii*) one root is imaginary and the other two are symmetric relative to the imaginary axis,

$$k_{\pm}^{(0)} = \pm k_R^{(0)} - i k_I^{(0)}, \quad (91)$$

$$k_3^{(0)} = i \kappa^{(0)}, \quad (92)$$

with real $k_{R,I}^{(0)}$ and $\kappa^{(0)}$ satisfying the conditions

$$\kappa^{(0)} - 2 k_I^{(0)} = \frac{1}{a_0} + \frac{r_0}{2} k_0^2, \quad (93)$$

$$k_R^{(0)2} + k_I^{(0)2} - 2 \kappa^{(0)} k_I^{(0)} = k_0^2, \quad (94)$$

$$\kappa^{(0)} \left(k_R^{(0)2} + k_I^{(0)2} \right) = \frac{k_0^2}{a_0}. \quad (95)$$

From these relations,

$$k_I^{(0)} \left[k_R^{(0)2} + \left(\kappa^{(0)} - k_I^{(0)} \right)^2 \right] = -\frac{r_0 k_0^4}{4}, \quad (96)$$

which shows that $k_I^{(0)} > 0$ for $r_0 < 0$. As before, the resonance poles are in the lower half of the complex momentum plane thanks to the renormalization constraint on the effective range for a non-ghost dimer field. In addition to the two resonance poles, the amplitude zeros induce an extra pole on the imaginary axis. In the $|k_0| \rightarrow \infty$ limit,

$$\lim_{|k_0| \rightarrow \infty} \kappa^{(0)} = \frac{r_0}{2} k_0^2, \quad (97)$$

while $k_{I,R}$ are given by Eqs. (23) and (24). Thus, for $|k_0| = \mathcal{O}(M_{hi})$ the additional pole represents a deep virtual (bound) state for k_0 real (imaginary). For the case considered here, $|k_0| = \mathcal{O}(M_{lo})$, it lies instead within the region of applicability of the theory. The S matrix now takes the form (5) with $N = 3$ ($n = \pm, 3$) and

$$\phi^{(0)}(k) = 0. \quad (98)$$

We can proceed to NLO as in the previous cases. The residual cutoff dependence of the LO amplitude is the same as in Eq. (26), indicating that LECs exist at NLO to remove it. A quick calculation shows that g_2 does not accomplish

this task in perturbation theory, and we can surmise that it is suppressed by the natural two powers of M_{hi} compared to g_0 . As in the case of a single shallow bound or virtual state [2–5], an enhanced C_0 requires an enhanced C_2 for renormalization at NLO. In addition to the LECs (27), we need

$$C_0^{(1)} = \mathcal{O}\left(\frac{1}{M_{hi}}\right), \quad C_2^{(1)} = \mathcal{O}\left(\frac{1}{M_{lo}^2 M_{hi}}\right). \quad (99)$$

The new interaction with LEC C_2 means that an additional parameter is introduced at NLO, which we can associate with a correction to the shape parameter (89).

These corrections lead to the NLO potential and amplitude shown in Figs. 11 and 12, which are the analogs of Figs. 2 and 3, respectively. They lead to

$$\begin{aligned} \frac{4\pi}{m} \left(\frac{T^{(1)}}{T^{(0)2}} - \delta T^{(1)-1} \right) &= \left[C_0^{(1)} \left(L_1 - \frac{1}{a_0} \right) + C_2^{(1)} L_3 - g_0^{(1)} \sqrt{-2mr_0} \right] \left(L_1 - \frac{1}{a_0} \right) - \frac{mr_0}{2} \Delta^{(1)} \\ &+ \left\{ C_0^{(1)} \left(L_1 - \frac{1}{a_0} \right) + \frac{C_2^{(1)}}{2} \left[L_3 + \frac{2}{r_0} \left(L_1 - \frac{1}{a_0} \right)^2 \right] \right. \\ &- \frac{g_0^{(1)}}{k_0^2} \sqrt{-\frac{2m}{r_0}} \left(L_1 - \frac{1}{a_0} + \frac{r_0 k_0^2}{2} \right) - \frac{m}{k_0^2} \Delta^{(1)} - \frac{L_{-1}}{r_0} \left. \right\} \frac{r_0 k^2}{1 - k^2/k_0^2} \\ &+ \left[\frac{C_0^{(1)}}{4} - \frac{C_2^{(1)}}{r_0^2 k_0^2} \left(L_1 - \frac{1}{a_0} \right) \left(L_1 - \frac{1}{a_0} - r_0 k_0^2 \right) \right. \\ &- \frac{g_0^{(1)}}{2k_0^2} \sqrt{-\frac{2m}{r_0}} - \frac{m}{2r_0 k_0^4} \Delta^{(1)} + \frac{L_{-1}}{r_0^2 k_0^2} \left. \right] \frac{r_0^2 k^4}{1 - k^2/k_0^2} \\ &+ \left[\frac{C_0^{(1)}}{4k_0^2} + \frac{C_2^{(1)}}{4} - \frac{g_0^{(1)}}{2k_0^4} \sqrt{-\frac{2m}{r_0}} - \frac{m}{2r_0 k_0^6} \Delta^{(1)} \right] \frac{r_0^2 k^6}{(1 - k^2/k_0^2)^2} \\ &- L_{-3} k^4 + \dots \\ &= - \left(P_0 + \frac{4}{r_0^2 k_0^2} \right) \left(\frac{r_0}{2} \right)^3 \frac{k^4}{1 - k^2/k_0^2} + \dots, \end{aligned} \quad (100)$$

where we imposed the renormalization conditions that no changes are induced in the energy dependence and parameters of the LO amplitude, other than the presence of a new term proportional to $P_0 - P_0^{(0)}$. This is accomplished with

$$C_2^{(1)}(\Lambda) = \frac{k_0^2}{(L_1 - 1/a_0 - r_0 k_0^2)^2} \left(\frac{r_0}{2} \right)^3 \left(P_0 + \frac{4}{r_0^2 k_0^2} + \frac{8L_{-1}}{r_0^3 k_0^2} \right), \quad (101)$$

$$C_0^{(1)}(\Lambda) = - \frac{k_0^2}{(L_1 - 1/a_0 - r_0 k_0^2)^3} \left(\frac{r_0}{2} \right)^3 \left\{ \left(P_0 + \frac{4}{r_0^2 k_0^2} \right) \left[L_3 - k_0^2 L_1 + \frac{k_0^2}{a_0} \left(1 - \frac{a_0 r_0 k_0^2}{2} \right) \right] + \frac{8L_{-1}}{r_0^3 k_0^2} (L_3 - r_0 k_0^4) \right\}, \quad (102)$$

$$\begin{aligned} g_0^{(1)}(\Lambda) &= - \left(-\frac{1}{2mr_0} \right)^{1/2} \frac{1}{(L_1 - 1/a_0 - r_0 k_0^2)^3} \left(\frac{r_0 k_0}{2} \right)^4 \left\{ \left(P_0 + \frac{4}{r_0^2 k_0^2} \right) \left[L_3 - \frac{2}{r_0} \left(L_1 - \frac{1}{a_0} \right) \left(L_1 - \frac{1}{a_0} + r_0 k_0^2 \right) \right] \right. \\ &\quad \left. + \frac{8L_{-1}}{r_0^3 k_0^2} \left[L_3 - 2k_0^2 L_1 + \frac{2k_0^2}{a_0} \left(1 - \frac{a_0 r_0 k_0^2}{4} \right) \right] \right\}, \end{aligned} \quad (103)$$

$$\Delta^{(1)}(\Lambda) = - \frac{L_1 - 1/a_0}{m(L_1 - 1/a_0 - r_0 k_0^2)^3} \left(\frac{r_0 k_0^2}{2} \right)^3 \left[\left(P_0 + \frac{4}{r_0^2 k_0^2} \right) \left(L_1 - \frac{1}{a_0} \right) + \frac{4L_{-1}}{r_0^2} \right]. \quad (104)$$

The NLO amplitude is then

$$T^{(0+1)}(k) = - \frac{4\pi}{m} \left[-\frac{1}{a_0} + \frac{r_0}{2} k^2 - \left(\frac{r_0}{2} \right)^3 \frac{P_0 k^4}{1 - k^2/k_0^2} - ik \right]^{-1} + \dots. \quad (105)$$

This result was obtained in Ref. [29] using two dimer fields, but we see here that no such complication is necessary.

The NLO corrections induce changes in the pole positions,

$$k_n^{(0+1)} = k_n^{(0)} \left[1 + i \left(P_0 + \frac{4}{r_0^2 k_0^2} \right) \left(\frac{r_0 k_n^{(0)}}{2} \right)^3 \frac{1 - k_n^{(0)2}/k_0^2}{(1 - k_n^{(0)2}/k_0^2)^2 + ir_0 k_n^{(0)}} \right], \quad (106)$$

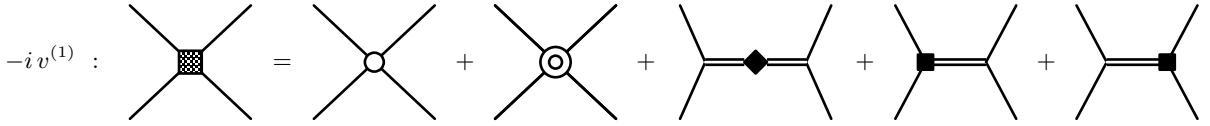


FIG. 11: Next-to-leading-order potential from the four-particle no-derivative (circle) and two-derivative contact interactions (circled circle), dimer residual mass (solid diamond), and two-particle/dimer coupling (solid square). Other symbols as in Fig. 1.

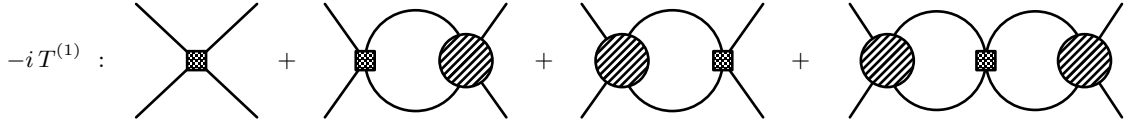


FIG. 12: Next-to-leading-order T matrix for a broad resonance in terms of the NLO potential (shaded square, Fig. 11) and the LO T matrix (Fig. 10).

and the background phase,

$$\phi^{(0+1)}(k) = - \left(P_0 + \frac{4}{r_0^2 k_0^2} \right) \left(\frac{r_0}{2} \right)^3 k_0^2 k. \quad (107)$$

In the limit $|k_0| \rightarrow \infty$ we regain Eqs. (33) and (34) for the two poles $n = \pm$. However, for $|k_0| = \mathcal{O}(M_{hi})$ the perturbative expansion for the $n = 3$ pole does not converge. As a consequence, the expansion for the phase does not commute with the $|k_0| \rightarrow \infty$ limit, and the three-pole $\phi^{(0+1)}(k)$ in Eq. (107) does not go into the two-pole Eq. (35).

Like in the case without a zero, the “...” in Eq. (105) contain terms $\propto \Lambda^{-3}$ indicating that new interactions appear at or before N^3LO , *e.g.* g_2 at N^2LO . We again stop at NLO although the procedure can be continued to higher orders if there is interest. There is no apparent obstacle to a consistent EFT formulation of a broad resonance with a low-energy amplitude zero based on the PC presented here. Yet, we have been unable to find an explicit potential-model realization of this idea. For example, we found no combination of α and β in the potential (70) that yields both a broad resonance and an amplitude zero. This is likely because there are not enough parameters to tune, but it leaves open the question of if (and how) this scenario can be realized.

VII. CONCLUSION

The existence of resonant poles in the scattering of two nonrelativistic particles requires a nonperturbative treatment of the dominant interactions between these particles, while a systematic expansion of the amplitude relies on distorted-wave perturbation theory being applied to subleading interactions. Following Refs. [9, 16], we investigated here a formulation of the low-energy effective field theory where the resonance poles enter through the propagation of a particle (dimer) with the resonance quantum numbers, described by its own field in the theory’s Lagrangian. The leading-order amplitude is indeed nonperturbative in a vicinity of the pole. In the case of a narrow resonance this region is small, and outside perturbation theory holds. A narrow resonance is naturally accompanied by a low-energy zero of the amplitude, which falls outside the nonperturbative region. In contrast, for a broad resonance the leading-order amplitude is nonperturbative in most of the region where the EFT applies. A low-energy zero of the amplitude appears only upon fine tuning.

We have explicitly constructed manifestly renormalized amplitudes for both broad and narrow resonances up to next-leading order in the EFT expansion. The case of a broad resonance without amplitude zero gives the amplitude obtained with only momentum-dependent interactions in Ref. [15]. When the zero is present, we provided an alternative derivation of the amplitude from Ref. [29], which employed two dimer fields and focused on three poles with imaginary momenta instead of a resonance. For a narrow resonance, we corrected the derivation of Ref. [14], which itself improved on Refs. [8, 13]. It would be interesting to build the equivalent EFT without a dimer field in the two cases where a zero is present.

The sign of the kinetic term for the dimer field is linked to the sign of the effective range. It has been shown [2–5] that positive effective range can be handled in an EFT with a ghost auxiliary field, as long as its kinetic term is treated perturbatively. The amplitude then has a single pole and cannot accommodate resonances. In all resonant cases, we took the kinetic term to have the usual sign associated with a positive-norm state. It is remarkable that, as for purely momentum-dependent interactions [15], renormalization of the leading-order amplitude requires the resonance poles

to be where they are expected by other arguments, namely on the lower half of the complex momentum plane. The subleading amplitudes can then be renormalized in (distorted-wave) perturbation theory and lead to small changes in the pole positions. We confirmed the improvement at next-to-leading order in the case of a narrow resonance using an explicit toy potential posing as underlying theory [13]. The same had previously been done for a broad resonance without amplitude zero [15], and we did not find a combination of potential parameters that gives rise to a low-energy amplitude zero.

We hope these ideas find application in the enormously rich physics of nuclear reactions, where resonances abound. In most situations, the Coulomb interaction must be added. Work in this direction is in progress, so as to extend the results of Refs. [10, 13] to more general cases.

Acknowledgments

UvK thanks Hans-Werner Hammer for discussions on the resummation of a negative dimer kinetic term. This research was supported in part by the U.S. Department of Energy, Office of Science, Office of Nuclear Physics, under award number DE-FG02-04ER41338.

[1] H.-W. Hammer, S. König, and U. van Kolck, Rev. Mod. Phys. **92** (2020) 025004.
 [2] U. van Kolck, Lect. Notes Phys. **513** (1998) 62.
 [3] D.B. Kaplan, M.J. Savage, and M.B. Wise, Phys. Lett. B **424** (1998) 390.
 [4] D.B. Kaplan, M.J. Savage, and M.B. Wise, Nucl. Phys. B **534** (1998) 329.
 [5] U. van Kolck, Nucl. Phys. A **645** (1999) 273.
 [6] U. van Kolck, Les Houches Lect. Notes **108** (2020) 362 [arXiv:1902.03141 [nucl-th]].
 [7] C.A. Bertulani, H.-W. Hammer, and U. van Kolck, Nucl. Phys. A **712** (2002) 37.
 [8] P.F. Bedaque, H.-W. Hammer, and U. van Kolck, Phys. Lett. B **569** (2003) 159.
 [9] D.B. Kaplan, Nucl. Phys. B **494** (1997) 471.
 [10] R. Higa, H.-W. Hammer, and U. van Kolck, Nucl. Phys. A **809** (2008) 171.
 [11] V. Pascalutsa and D.R. Phillips, Phys. Rev. C **67** (2003) 055202.
 [12] B. Long and U. van Kolck, Nucl. Phys. A **840** (2010) 39.
 [13] B.A. Gelman, Phys. Rev. C **80** (2009) 034005.
 [14] M.H. Alhakami, Phys. Rev. D **96** (2017) 056019.
 [15] J.B. Habashi, S. Fleming, S. Sen, and U. van Kolck, Annals Phys. **422** (2020) 168283.
 [16] S. Weinberg, Phys. Rev. **130** (1963) 776.
 [17] P.F. Bedaque and H.W. Grießhammer, Nucl. Phys. A **671** (2000) 357.
 [18] N. Hu, Phys. Rev. **74** (1948) 131; (E) **75** (1949) 75.
 [19] R.E. Peierls, Proc. Roy. Soc. (London) A **253** (1959) 16.
 [20] R.G. Newton, J. Math. Phys. **1** (1960) 319.
 [21] U. van Kolck, Eur. Phys. J. A **56** (2020) 97.
 [22] C.W. Ramsauer Ann. Phys. **396** (1921) 513.
 [23] J.S. Townsend and V.A. Bailey, Phil. Mag. **43** (1922) 593.
 [24] C. Møller, Kgl. Danske Vid. Selsk. Mat.-Fys. Medd. **22** (1946) 19.
 [25] W. Schützer and J. Tiomno, Phys. Rev. **83** (1951) 249.
 [26] S.R. Beane and M.J. Savage, Nucl. Phys. A **694** (2001) 511.
 [27] F. Gabbiani, arXiv:nucl-th/0009072 [nucl-th].
 [28] N.G. van Kampen, Phys. Rev. **91** (1953) 1267.
 [29] M. Sánchez Sánchez, C.-J. Yang, B. Long, and U. van Kolck, Phys. Rev. C **97** (2018) 024001.
 [30] G. Rupak, A. Vaghani, R. Higa, and U. van Kolck, Phys. Lett. B **791** (2019) 414.
 [31] E. Braaten, M. Kusunoki, and D. Zhang, Annals Phys. **323** (2008) 1770.
 [32] S. Diehl and C. Wetterich, Phys. Rev. A **73** (2006) 033615.